TIME-DEPENDENT RELIABILITY ANALYSIS OF MASONRY PANELS UNDER HIGH PERMANENT COMPRESSIVE STRESSES

J.J. Kim[1] and M.M. Reda Taha[2]
[1]Post Doctor Fellow, Dept. of Civil Engineering, University of New Mexico, Albuquerque, USA,
E-mail:jjkim@unm.edu
[2]Associate Professor and Regents' Lecturer, Dept. of Civil Engineering,
University of New Mexico, Albuquerque, USA,
E-mail:mrtaha@unm.edu

ABSTRACT
The collapse of historical masonry structures in Europe in the late 1990's raised the interest in understanding the long-term effect of masonry under sustained compressive stresses. That requires combining the significance of time-dependent effects of creep with the effect of damage due to overstress to realize the evolution of cracks and then failure in masonry. Meanwhile, composite analysis of masonry panels was proven effective for realizing ultimate strength capacity. Composite analysis also provides the ability to consider system reliability in analyzing masonry panels.
In this article, a masonry panel under high compressive stress to strength ratio is considered. The panel is modelled as a composite structure by considering a repeated unit cell of mortar and brick. Load redistributions due to creep in mortar and brick as composite materials are accounted for. A step-by-step in time analysis is performed to track the load redistribution in the composite masonry. Time-dependent system reliability analysis of the masonry panel is performed by defining component and system limit state functions at each time step.

KEYWORDS: reliability, masonry, creep, composite.

INTRODUCTION
Creep strain is defined as the strain increment observed over time in materials subject to sustained stress [1]. Creep is known for its effect on serviceability of structures. In composite structures consisting of more than two bonded materials, loads are distributed to individual material according to its relative stiffness and end constraints with other materials [1]. Therefore, creep can produce significant stress redistribution within the composite material affecting the composite action [2, 3]. Shrive [4] demonstrated the significance of creep on prestress loss in post-tensioned masonry. Moreover, investigations after the collapse of the Civic Tower in Pavia in Italy revealed that the historic masonry structure collapsed under sustained loads that were close to 60% of its ultimate capacity [5]. Creep experiments on clay masonry showed that creep deformation significantly contributes toward the total deformation and can lead to structural

failure [6]. Numerous efforts for predicting and modelling creep in structural masonry have been reported by several researchers [6-8].

In this study, a masonry panel is modelled as a composite structure including mortar and brick as suggested by Shrive and England [9]. We show that creep redistributes load between brick and mortar by constraints without additional loading. A step-by-step in time analysis [10] is used to determine time-dependent reliability incorporating composite action. By assuming mortar and brick as brittle or perfectly plastic materials, the bounds of reliability indexes are determined. We then determine the reliability indexes for quasi-brittle masonry as an intermediate state between brittle and ductile behaviours. Failure criteria for the composite model are derived using *De Morgan's principles* [11]. A case study is presented using the step-by-step method considering specific creep models for mortar and brick. The results show the significance of creep on reliability of masonry panels under sustained axial loads.

METHODS

The '*violation*' of a limit state can be defined as the attainment of undesirable conditions of structures [12]. For a structure that has the resistance R(X) and is subjected to the load effect P(X), the limit state function for a set of uncertain variables X can be defined as

$$G(\mathrm{X}) = R(\mathrm{X}) - P(\mathrm{X}) \quad \text{where} \quad \mathrm{X} = \{x_1, x_2, ..., x_n\} \tag{1}$$

In this case, the violation of limit state will take place when '$G(\mathrm{X}) \leq 0$' and the integration of joint probability density function (PDF) of variables x for the violation region results in the probability of failure of the structure. Therefore, for linear limit state function and normal joint PDF of variables x, the probability of failure can be represented by the well known reliability index β representing the normal distance from the origin of the standard joint PDF to the limit state function computed using the first two moments, mean and standard deviation, of joint PDF

$$\beta = \frac{\mu_R - \mu_P}{\sqrt{\sigma_R^2 + \sigma_P^2}} \tag{2}$$

where μ_R, μ_P, σ_R and σ_P are the means and the standard deviations of R and P respectively, which are propagated from the means and the standard deviations of variables x. The probability of failure can be determined as

$$p_f = \Phi^{-1}(-\beta) \tag{3}$$

where Φ^{-1} is the inverse of standard normal cumulative density function (CDF). Considering the *central limit theorem*, if a first order approximation of nonlinear limit state function can be attained, the reliability index can be used to calculate the probability of failure. An acceptable reliability index β is used to determine the load and resistance factors for design codes [13].

System reliability analysis

The structural unit element in a masonry panel can be defined using a repeated unit cell/element shown in Figure 1 (a) [8]. This unit element is made up of two parallel composite parts that consist of mortar and brick as shown in Figure 1 (b). It is assumed that displacement compatibility is satisfied at the top and the bottom of the unit element. In other words, bond between the two parts in the unit element is considered to be perfect bond during analysis to ensure shear force between two parts are transferred.

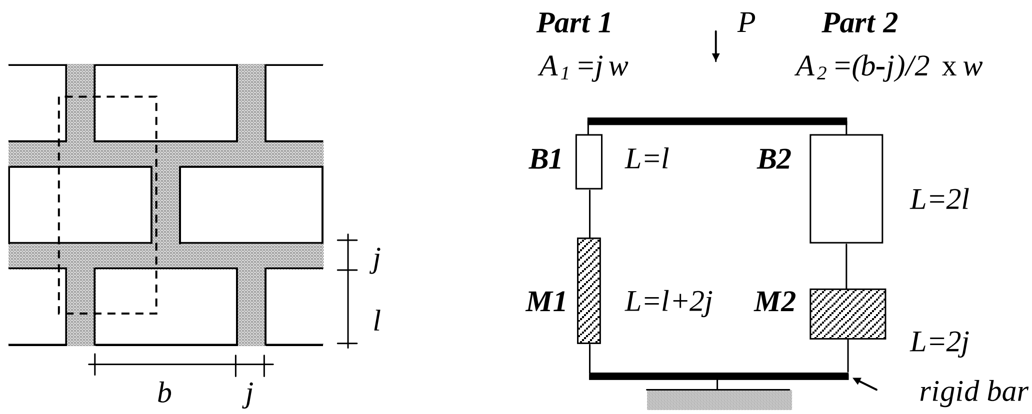

(a) Repeated unit cell in masonry panel **(b) Unit element**

Figure 1: (a) Repeated unit cell (inside of broken line) in masonry panel which thickness is *w* and (b) modeling reapeated unit cell as unit element

As shown in Figure 1 (b), the suggested unit element can be considered as a set structure. The unit element in Figure 1 (b) can resist loads until both parts of the unit element fail. Moreover, if either mortar or brick fails in a part, that part cannot resist loads. Therefore, a survival set of the unit element S can be expressed by operations on classical set theory, *union* and *intersection* as

$$S = (BS_1 \cap MS_1) \cup (BS_2 \cap MS_2) \qquad (4)$$

where

BS_1 = survival of *B1* (brick in *Part 1*), MS_1 = survival of *M1* (mortar in *Part 1*)
BS_2 = survival of *B2* (brick in *Part 2*), MS_2 = survival of *M2* (mortar in *Part 2*)

To describe the failure criteria, the failure set of the unit element F can be taken as the complement of the survival set of the unit element S and it is shown as

$$F = \overline{(BS_1 \cap MS_1) \cup (BS_2 \cap MS_2)} \qquad (5)$$

where the over-line symbol of each set denotes the complement of the set. Using *De Morgan's principle*, Eq. (5) will be re-written as

$$F = (\overline{BS_1} \cup \overline{MS_1}) \cap (\overline{BS_1} \cup \overline{MS_1}) \qquad (6)$$

As both mortar and brick can be considered as quasi-brittle materials, both materials can maintain some load after cracking (considered here as failure). For parallel system of brittle materials, if one part fails, that part cannot resist load anymore and the whole load transfers to

the other part. However, for parallel system of perfectly plastic materials, if one part fails, that part can maintain the amount of its maximum load capacity and the remaining load transfers to the other part. Therefore, by assuming mortar and brick as brittle or perfectly plastic materials, the upper and lower bounds of the reliability index can be determined.
First, assuming both mortar and brick are perfectly plastic materials, the reliability index β_d for ductile behavior of Eq. (6) can be calculated after [14]

$$\beta_d = \Phi\left[\left\{1-(1-p_{f,M1})(1-p_{f,B1})\right\}\left\{1-(1-p_{f,M2})(1-p_{f,B2})\right\}\right] \tag{7}$$

where $p_{f,M1}$, $p_{f,B1}$, $p_{f,M2}$ and $p_{f,B2}$ are the probabilities of failure calculated using Eqs. (2) and (3) considering the maximum strengths and the applied stresses of mortar and brick in each part. Second, if we assume that both mortar and brick are brittle, the reliability index β_b for brittle materials can be calculated with the overall resisting force for the unit element $R_{\max}$ defined after [14] as

$$\beta_b = \frac{R_{\max} - P}{\sqrt{\sigma_{R_{\max}}^2 + \sigma_P^2}} \tag{8}$$

where $R_{\max} = \max\left[\min\left\{2 f_m jw,\ 2 f_b jw\right\},\ \min\left\{f_m(b-j)w/2,\ f_b(b-j)w/2\right\}\right] \quad for \quad b > 3j$ (9)

where P is the load applied to the system in Figure 1 (b). $\sigma_{R\max}$ and σ_P are the standard deviations of $R_{\max}$ and P respectively. Finally, the reliability index for quasi-brittle materials denoted β_q shall lie between the upper and lower bounds of the reliability indexes defined above such that

$$\beta_b < \beta_q < \beta_d \tag{10}$$

It is noticeable that while the reliability index of ductile materials depends on the load level in each part, the reliability index of brittle materials depends on only the overall load. With the reliability index of quasi-brittle material β_q being between these two bounds, the reliability index of quasi-brittle materials depends on both the load level in each part and the overall load.

Composite materials incorporating creep

When axial load P applies to a composite structure consisting of two parts bonded in parallel at time t, force equilibrium at time t requires

$$P(t) = P_1(t) + P_2(t) \tag{11}$$

where $P_1(t)$ and $P_2(t)$ are the forces acting on *Part 1* and *2* at time t respectively. Moreover, when additional deflection by creep is incorporated to each material, compatibility condition at time t requires

$$P_1(t)/K_1(t) + \Delta_{creep,1}(t) = P_2(t)/K_2(t) + \Delta_{creep,2}(t) \tag{12}$$

where $K_1(t)$ and $K_2(t)$ denote stiffness of *Part 1* and *2* at time *t* respectively. $\Delta_{creep,1}(t)$ and $\Delta_{creep,2}(t)$ are additional creep deflection of *Part 1* and *2* at time *t* respectively. Although the additional creep deflection at time *t* can be determined by both the effective modulus method and the step-by-step method, the step-by-step method was used to avoid missing stress peak [15]. The main idea of the step-by-step in time method is that both force equilibrium in Eq. (11) and compatibility condition in Eq. (12) are satisfied at the end of each time step. For the first time step, initial value of applied load for each part can be calculated using the elastic solution. For the masonry panel as shown in Figure 1 (b), stiffness of both parts, $K_1(t)$ and $K_2(t)$ will be calculated as

$$1/K_1(t) = \left[\left(l+2j\right)/E_m(t) + l/E_b(t)\right]/jw \tag{13}$$

$$1/K_2(t) = 2\left[j/E_m(t) + l/E_b(t)\right]/[(b-j)w/2] \tag{14}$$

where $E_m(t)$ and $E_b(t)$ are modulus of elasticity of mortar and brick at time *t* respectively. *b*, *l* and *w* denote brick size and *j* is mortar thickness as shown in Figure 1 (a). Additional creep deflection of each part during a time step is determined with assumption that the load at the beginning of the time step remains constant during the time step. Therefore, creep deflection of each part for *n*-th time step will be

$$\delta\Delta_{creep,1}(n) = \frac{P_1(n-1)}{jw}\left\{\delta sc_m(n)\times(l+2j) + \delta sc_b(n)\times l\right\} \tag{15}$$

$$\delta\Delta_{creep,2}(n) = \frac{P_2(n-1)}{(b-j)w/2}\left\{\delta sc_m(n)\times 2j + \delta sc_b(n)\times 2l\right\} \tag{16}$$

where $P_1(n\text{-}1)$ and $P_2(n\text{-}1)$ denote the forces that are redistributed at the end of previous time step. δsc_m and δsc_b are the specific creep increments of mortar and brick respectively for the time step. Therefore, if *n* time steps are used until time *t*, total creep deflections at time *t* will be represented as accumulation of the number of *n* creep deflections such as

$$\Delta_{creep,1}(t) = \sum_{i=1}^{n} \delta\Delta_{creep,1}(i) \tag{17}$$

$$\Delta_{creep,2}(t) = \sum_{i=1}^{n} \delta\Delta_{creep,2}(i) \tag{18}$$

By using Eqs. (11) to (18), overall behaviour of masonry including creep can be demonstrated. If we consider continuum damage in either component as a function of time, the loads redistributed to each part can be determined. Because stiffness at time *t* in Eqs. (13) and (14) would vary with respect to time [16]. On the other hand, if all material components stayed in elastic stress region for service load level, $E_m(t)$ and $E_b(t)$ in Eqs. (13) and (14) can be treated as constant as E_m and E_b respectively. Therefore, Eqs. (11) to (18) can be solved for stress in *Part 2* as

$$\sigma_2(t) = \left[\sigma(t)\left\{1+s_2\right\} - 2g\,E_b\,DSC(t)/jc\right]/\left[4g+h\right] \tag{19}$$

where, $\sigma(t)$ is total applied stress at time t, $\sigma_2(t)$ is applied stress to *Part 2* at time t and the parameters in Eq. (19) are defined as

$c = E_{b,ini} / E_{m,ini}$, $s_1 = l / j$, $s_2 = b / j$, $g = \dfrac{c}{cs_1 + 2c + s_1}$, $h = \dfrac{4gs_1}{c} + s_2 + 1$ and $DSC(t) = \Delta_{creep,2}(t) - \Delta_{creep,1}(t)$. After $\sigma_2(t)$ is determined using Eq. (18), $\sigma_1(t)$ can be identified using Eq. (11).

CASE STUDY

A case study for time-dependent reliability analysis of masonry is examined and presented here. A standard masonry panel was chosen [17]. Clay brick size was chosen as its dimension b x l x w of 190 x 57 x 90 mm. Mortar joints were chosen as 10 mm thick. The maximum strengths of mortar and brick were used as 10 MPa and 50 MPa respectively. Constant load during analysis was applied for case study as shown in Figure 2 (a). For reliability analysis, load variation at time t was assumed as 5%. The maximum strength variations for mortar and brick were used as 15% and 5% respectively. The properties of brick and mortar for analysis are presented in Table 1 with the calculated constants for the step-by-step analysis.

Table 1: Input and calculated constants for case study

Material properties and geometries		Calculated constants	
b	190 mm	$c=E_b/E_m$	3
l	57 mm	$s_1=l/j$	5.7
w	90 mm	$s_2=b/j$	19
j	10 mm	g	0.104
$f_{m,max}$	10 MPa	h	9.396
$f_{b,max}$	50 MPa	$\sigma_1(0)$	4.11 MPa
E_m	3.33 GPa	$\sigma_2(0)$	6.77 MPa
E_b	10.0 GPa	*Elastic strain*	879 μ

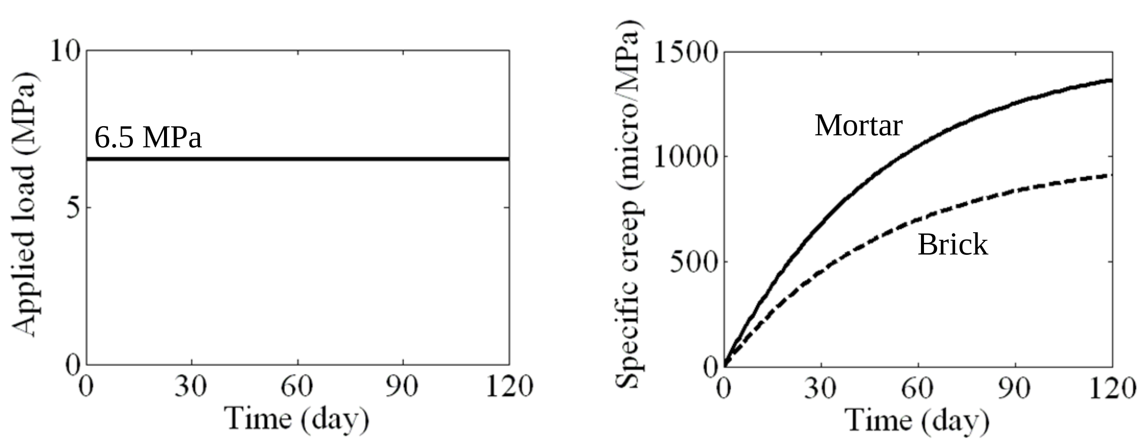

(a) Applied load **(b) Specific creep models for mortar and brick**

Figure 2: Input data used for case study

Specific creep is defined as

$$sc(t) = M\left(1 - e^{-\frac{t}{T}}\right) \quad [\text{microstrain} / \text{MPa}] \tag{20}$$

where $sc(t)$ is specific creep at time t. M and T are constant. The constant M and T in Eq. (20) for mortar were chosen as 1500 and 50 respectively [16]. Specific creep for brick was assumed as two third of that of mortar. The specific creep for mortar and brick are shown in Figure 2 (b).

RESULTS AND DISCUSSION

The change in stress with respect to time in each part of the unit element is presented in Figure 3. While stress in *Part 1* increases, stress in *Part 2* decreases by composite action. Based on these stress change, the reliability index for plastic materials is calculated at each time step by Eq. (7). On the other hand, there is no contribution of composite action to the reliability index for brittle materials. The reliability indexes for plastic materials at initial loading time in Eq. (21) and for brittle materials in Eqs. (22) and (23) are calculated as

$$\beta_d = \Phi\left[\left\{1-(1-0.00013)(1-4\times10^{-75})\right\}\left\{1-(1-0.0372)(1-4\times10^{-66})\right\}\right] = 4.42 \tag{21}$$

$$\beta_b = (81-58.5)/\sqrt{(81\times0.15)^2 + (58.5\times0.05)^2} = 1.8 \tag{22}$$

$$\text{where} \quad R_{\max} = \max\left[\min\{18,\ 90\},\ \min\{81,\ 405\}\right] = 81\text{kN} \ \ (\mathit{for} \ \ b = 190 > 3j = 30) \tag{23}$$

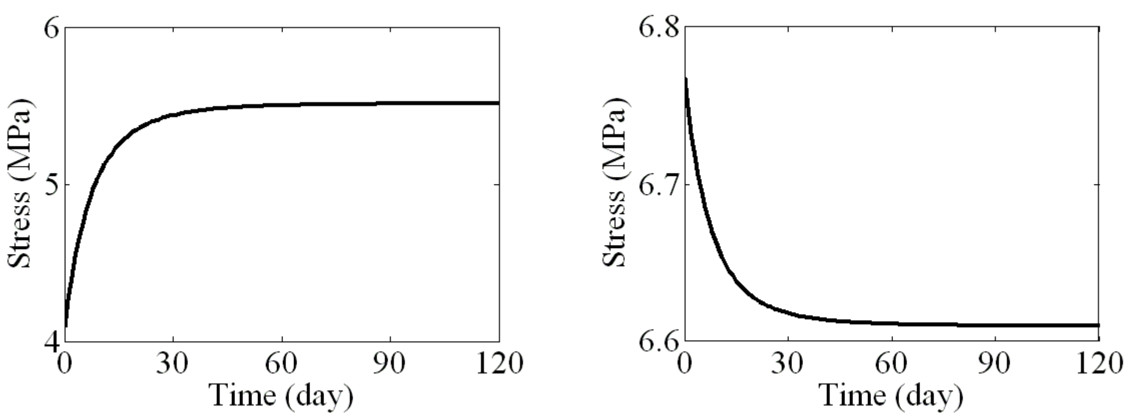

(a) ***Part 1*** **(b)** ***Part 2***

Figure 3: Change of stress in each part of the unit element with respect to time

The reliability indexes for ductile and brittle materials are shown as the upper and the lower bounds with respect to time in Figure 4. The reliability index for quasi brittle material can be determined by identifying the level of ductility of the quasi-brittle material. For the case study, as brick is relatively stronger than mortar, the probability of failure of brick in both parts of the unit element is negligible as demonstrated by Eq. (21). Therefore, the overall reliability of masonry panel depends on the reliability of mortar. Conclusively, the reliability of masonry panel for our case study is determined by considering the level of ductility in mortar.

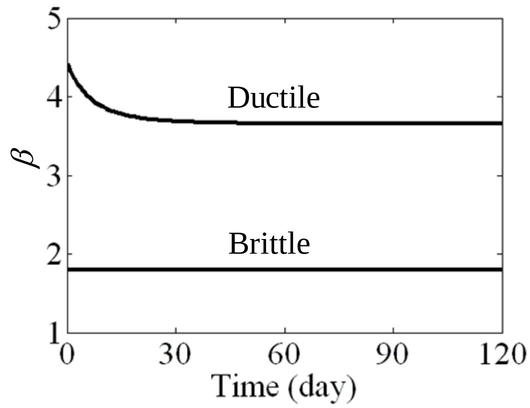

Figure 4: Reliability index bound with respect to time

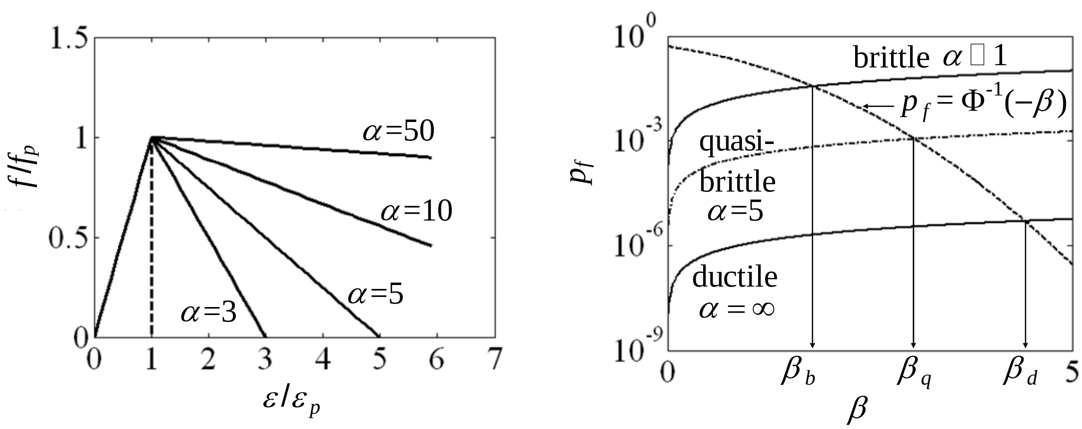

(a) Linear decsending stress strain curves **(b) Interpolation curves**

Figure 5: Interpolation of the reliability index with respect to ductile behaviour

By considering linear descending stress-strain relationship after Scanlon and Murray [18],

$$f / f_p = \frac{1}{(1-\alpha)}\left[(\varepsilon / \varepsilon_p) - \alpha\right] \quad \text{for } \varepsilon / \varepsilon_p > 1 \text{ and } \alpha > 1 \tag{24}$$

where α is the maximum to peak strain ratio. As shown in Figure 5 (a) for various cases of α, the maximum to peak strain ratio α is related to ductility of mortar. Therefore, a ductility number λ can be defined as

$$\lambda = 1 - \exp\left[-\omega(\alpha - 1)^{\zeta}\right] \tag{25}$$

where ω and ζ are constants to relate the ductility number λ to the maximum to peak strain ratio α. Here, we use ω and ζ equal unity respectively. Moreover, the intermediate reliability index for quasi-brittle material can be found by considering an intermediate probability of failure between ductile and brittle probability of failures. Therefore, it is suggested to use the probability of failure to reliability index ratio γ defined as

$$\gamma = p_f / \beta \quad \text{thus} \quad \Phi^{-1}(-\beta) - \gamma\beta = 0 \tag{26}$$

The interpolation for quasi-brittle material γ_q is computed as

$$\gamma_q = \lambda\gamma_d + (1-\lambda)\gamma_b \tag{27}$$

The graphical representation of interpolation for α equals 5 is shown in Figure 5 (b).

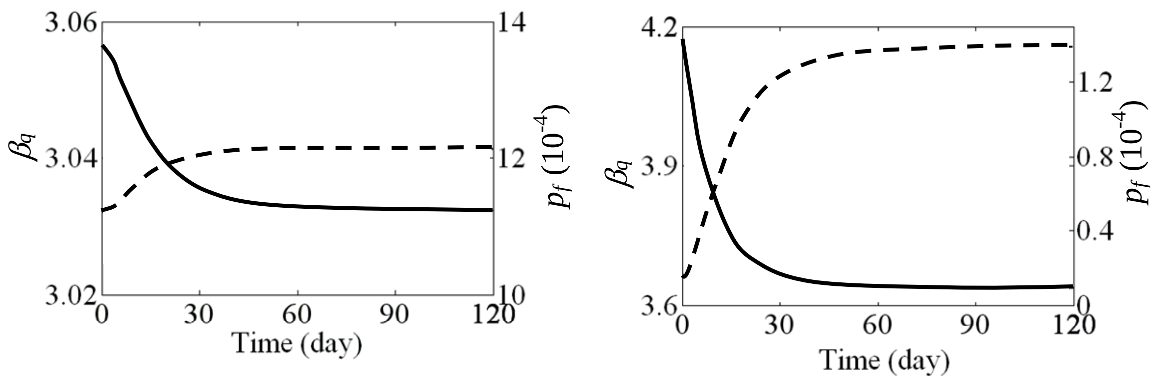

(a) α=5 **(b) α=10**

Figure 6: Reliability index (solid line) and probability of failure (broken line) for masonry panel when its mortar stress-strain curve for α values as (a) 3 or (b) 5

The interpolated reliability index β_q and probability of failure $p_{f,q}$ for quasi-brittle masonry are presented in Figures 6(a) and (b) for two different values of α. The results show that the reliability of masonry panel under sustained load decreases with time. It is noticeable that as the ductility of the quasi-brittle material increases due to a confining stress effects on materials [19], a modification of the ductility number λ for mortar, which lie in the tri-axial compressive stress state [20], will be needed.

CONCLUSION

Reliability analysis for masonry panels was conducted by modelling repeated unit element of a masonry panel as a system unit cell. The reliability index of quasi-brittle materials were interpolated from the reliability indices of brittle and ductile materials by considering ductile behaviour of masonry. A case study of a masonry panel under relatively high permanent compressive stresses is considered. The results of the case study show that load redistribution caused by creep can alter the level of structural reliability of masonry panels under permanent stress. The results also indicate that ductility of mortar joints has a major effect on masonry panel reliability (*probability of failure*) and its change with time due to creep. It is concluded that the significance of triaxial confinement of mortar joints on mortar joint ductility shall be considered when analyzing time-dependent reliability of masonry panels. Further research is underway to incorporate that effect.

REFERENCES

1. Ghali, A. And Favre, R., *Concrete Structures : Stresses and Deformation*, 2nd Ed., E$FN SPON, London, UK, 1994.
2. Neville, A. M., Dilger, W. H. And Brooks, J.J., *Creep of Plain and Structural Concrete*, 1st Ed., Construction Press, UK, 1983.
3. Lenczner, D., Creep in model Brickwork, *Proceedings of Designing Engineering and Construction with Masonry Products,* Johnston, F.B. Houston, U.S.A., pp. 58-67, 1969.
4. Shrive, N. G., Effects of Time Dependent Movements in Composite and Post-tensioned Masonry, *Masonry International*, 2, pp. 25, 1988.
5. Binda, L., Anzani, A. and Gioda, G., An Analysis of The Time-Dependent Behaviour of Masonry Walls, *Brick and Block Masonry*, 2, pp. 1058-1067, 1991.
6. Shrive, N. G., Sayed-Ahmed, E. Y. and Tilleman, D., Creep Analysis of Clay Masonry Assemblages, *Canadian Journal of Civil Engineering*, 24, pp. 367-379, 1997.
7. Reda Taha, M. M., Noureldin, A., El-Sheimy, N. and Shrive, N. G., Artificial Neural Networks for Predicting Creep with An Example Application to Structural Masonry, *Canadian Journal of Civil Engineering*, 30, pp. 523-532, 2003.
8. Van Zijl, G.P.A.G. *A Numerical Formulation for Masonry Creep, Shrinkage and Cracking*. Series 11, Engineering Mechanisms 01, Delft University Press, The Netherlands, 1999.
9. Shrive, N. G. and England, G. L., Elastic, creep and shrinkage behaviour of masonry, *International Journal of Masonry Construction*, 1, pp. 103-109, 1981.
10. England, G. L., Steady-State Stresses in Concrete Structures Subjected to Sustained Loads and Temperatures, *Parts I and II. Nuclear Engineering and Design*, 3, pp. 54-65 & 246-255.
11. Ross, T. J., *Fuzzy Logic with Engineering Applications*, 2nd Ed., WILEY, NJ, USA, 2004.
12. Melchers, R.E., *Structural Reliability Analysis and Prediction*, Second Edition, USA, John Wiley & Sons, 1999.
13. MacGregor, J. G., Safety and Limit States Design for Reinforced Concrete, *Canadian Journal of Civil Engineering*, 3, pp. 484-513, 1976.
14. Nowak, A. S. and Collins, K., *Reliability of Structures*, USA, McGraw Hill, 2000.
15. Reda Taha, M. M. and Shrive, N. G., A Model of Damage and Creep Interaction in A Quasi-Brittle Composite Material Under Axial Loading, *J. of Mechanics*, 22, pp. 339-347, 2006.
16. Kim, J. J. and Reda Taha, M.M., Integrating Creep and Damage in Modeling Historical Masonry: A Numerical Investigation, *Proc. of 5th ASCE International Engineering and Construction Conference (IECC'5)*, Irvine, CA, pp. 291-297, 2008.
17. Glanville, J.I., Hatzinikolas, M.A. and Ben-Omran, H.A., *Engineered Masonry Design, limit States Design*, Canada, Winston House, 1996
18. Scanlon, A. and Murray, D. W., Time Dependent Reinforced Concrete Slab Deflections, *Journal of the Structural Division* 100 (ST9) ASCE, pp. 1911-1924, 1974.
19. MacGregor, J. G. and Wight, J. K., *Reinforced Concrete: Mechanics and Design*, 4th Ed., Pearson Prentice Hall, NJ, USA, 2005.
20. Massart, T. J., Peerlings, R. H. J., Geers, M. G. D. and Gottcheiner, S., Mesocopic Modeling of Failure in Brick Masonry Accounting for Three-Dimensional Effects, *Engineering Fracture Mechanics*, 72, pp. 1238-1253, 2005.